A Journal of the Gesellschaft Deutscher Chemiker

Angewandte International Edition

GDCh

Chemie

www.angewandte.org

Accepted Article

Title: Perfluorinated Covalent Triazine Framework for High-selectivity Electroconversion CO2 into CH4

Authors: Yuanshuang Wang, Junxiang Chen, Genxiang Wang, Yan Li, and Zhenhai Wen

To be cited as: *Angew. Chem. Int. Ed.* 10.1002/anie.201807173
Angew. Chem. 10.1002/ange.201807173

Link to VoR: http://dx.doi.org/10.1002/anie.201807173
http://dx.doi.org/10.1002/ange.201807173

WILEY-VCH

10.1002/anie.201807173

WILEY-VCH

Perfluorinated Covalent Triazine Framework Derived Hybrids for High-selectivity Electroconversion CO_2 into CH_4

Yuanshuang Wang[a] +, Junxiang Chen[a] +, Genxiang Wang[a] +, Yan Li[a], Zhenhai Wen[a]*

Abstract: Developing cost-effective electrocatalysts for high-selectivity CO_2 electroreduction remains a daunting challenge. We here report a perfluroinated covalent triazine framework (CTF) electrocatalyst that holds an impressive high selectivity towards CO_2 electroreduction conversion into CH_4 with faradaic efficiency of 99.3% in aqueous electrolyte. Systematic characterization and electrochemical study, coupling with density functional theory calculations, demonstrate that co-covalent of nitrogen and fluorine in CTF provides a unique pathway that is inaccessible with the individual components for CO_2 electroreduction, contributing to the catalytic sites with high selectivity for CO_2 conversion into CH_4.

Fossil fuels have become the major energy sources to meet the global energy demands for economic and social development since the industrial revolution. The excessive consumption of fossil fuels would discharge the vast amount of CO_2 that could destruct the carbon cycle among ocean, land, and atmosphere, causing the enormous worries on the emerged global warming issues.[1] It is thus highly desirable to develop an effective strategy or technique to re-balance the carbon cycle by reducing the amount of CO_2 in the atmosphere. Electrochemical reduction of CO_2 has been regarded as a promising route to recycle CO_2 into value-added fuels and chemicals with harnessing electricity generated from renewable energy sources (*e.g.,* windy, solar).[2] Therefore, tremendous efforts have been put into exploring efficient electrocatalysts, including a variety of transition metal and their complexes, and metal free carbon materials are promising candidates.[3] Nevertheless, we still must strive to develop robust electrocatalysts that can highly selectively reduce CO_2 in aqueous electrolyte.[2d, 4]

Recently, covalent triazine framework (CTF), due to its ultralarge surface area, has received tremendous attentions for a variety of potential applications in the fields of catalytic supports, gas capture and storage, energy conversion and storage, optoelectronics and semiconductors.[5] Moreover, it is rather convenient to tune heteroatom doping in CTF by using heteroatom-containing molecular building-block as resource,[6] offering the possibility for developing CTF evolved materials as tunable electrocatalysts for CO_2 reduction. Unfortunately, the metal-free CTF based materials as CO_2 reduction electrocatalyst is rarely reported so far although highly deserved.

We herein report the synthesis of perfluorinated covalent triazine framework (FN-CTF-400) with the ionothermal assistance of molten $ZnCl_2$ at 400°C by using tetrafluoroterephthalonitrile as source.[6h] For comparison, a series of nitrogen and fluorine co-doped carbon (FN-CTF-X, X represent the synthetic temperature) were prepared by further treatment of FN-CTF-400 at different temperature, and nitrogen and chlorine co-doped CTF (ClN-CTFs) were prepared using the same method by using F-free precursors (Supporting Information, Figure S1).[6g]

The synthesis process is schematically described in Figure 1a, in which the FN-CTF-400 samples were prepared by a one-step polymerization with the assistance of $ZnCl_2$. The morphologies were examined by scanning electron microscopy (SEM) and transmission electron microscopy (TEM). One can see the FN-CTF-400 holds a three-dimensional (3D) structure with interconnected polymer framework according to the SEM image (Figure 1b) and a large amount of micropores based on TEM observation (Figure 1c). The high resolution TEM (HRTEM) image for the FN-CTF-400 is displayed in Figure 1d, revealing the sparse crystalline lattice with space of ~0.39 nm, as evidenced by the corresponding intensity profile for the line scan across the lattice fringes (inset of Figure 1d). The single graphitic layers are seen to be bending likely due to the fluorine and nitrogen doping.[7] And the energy dispersive X-ray spectroscopy (EDS) elemental map indicates that N and F are homogeneously distributed on the entire structure (Figure 1e and Figure S2). The morphologies for the other counterpart samples were also characterized with displaying similar morphology to the FN-CTF-400 (Figure S3).

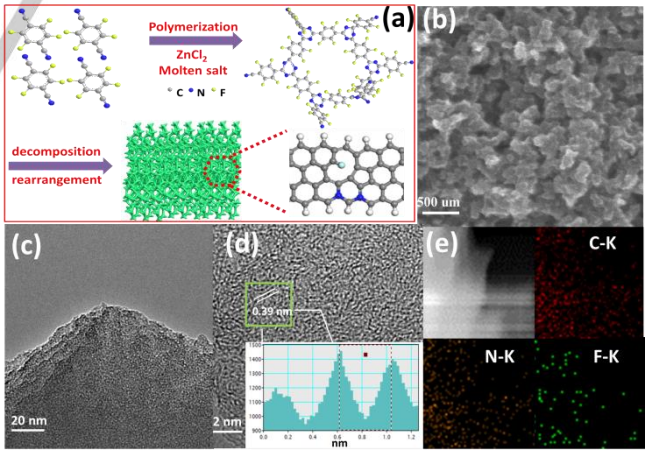

Figure 1. (a) Reaction schemes and the structure of the FN-CTF-400; (b) SEM image of FN-CTF-400; (c) TEM image and (d) HRTEM image with corresponding intensity profile for the line scan across the lattice fringes of the FN-CTF-400; (e) the EDS elemental mapping of the FN-PCTF-400.

The samples were also studied using a variety of techniques, including X-ray power diffraction (XRD), Raman spectra, X-ray photoelectron spectroscopy (XPS), and N_2 adsorption/desorption. XRD patterns for the FN-CTF-400 and the CTF derived materials (*i.e.,* FN-CTF-550, FN-CTF-700 FN-CTF-900) exhibit two weak and broad peaks (Figure S4), implying its poor crystallinity. Raman spectra of the FN-CTFs samples obtained at different temperature were performed to further study the local

[a] Y. S. Wang, J. X. Chen, G. X. Wang, Y. Li, and Prof. Dr. Z. H. Wen
CAS Key Laboratory of Design and Assembly of Functional Nanostructures, Fujian Provincial Key Laboratory of Nanomaterials, Fujian Institute of Research on the Structure of Matter, Chinese Academy of Sciences
Fuzhou 350002, P. R. China
E-mail: wen@fjirsm.ac.cn
+ These authors contributed to this work equally

Supporting information for this article is given via a link at the end

disorder and crystallinity. The intensity ratio of peaks for structure defects (I_D) and crystalline graphitic carbon (I_G) in the samples enhance slightly with decreasing temperature (Figure 2a), suggesting the samples obtained at increased temperature likely decrease the defects of samples. Additionally, the elemental composition, chemical state and electronic state of the elements of the FN-CTFs samples were investigated by X-ray photoelectron spectroscopy (XPS). Figure 2b displays the survey XPS spectra for the set of FN-CTFs samples. The FN-CTF-400 manifests an eye-catching signal at 686.04 eV corresponding to F1s,[6h] and the FN-CTF-550 presents a significant decrease in F1s peak intensity, while the FN-CTF-700 and the FN-CTF-900 notably show no F1s peak. Moreover, with the increased synthetic temperature, the FN-CTFs samples display distinctly decrease in intensity for N1s accompanying with the increase in intensity for C1s, which indicate that increasing temperature would diminish the doping level of heteroatom, being consistent with the decreased defects density verified by Raman analysis. We made a further analysis on the high resolution XPS spectrum of N1s and F1s for the FN-CTFs (Figure 2c-d and Figure S5). The F1s spectra for the FN-CTF-400 (Figure 2d) can be deconvoluted into two component peaks at 687.3 and 690.0 eV, corresponding to covalent C-F and semi-ionic C-F, respectively,[8] while there are no signals of F element in XPS spectra of FN-CTF-700 and FN-CTF-900 (Figure S5d and 5f).

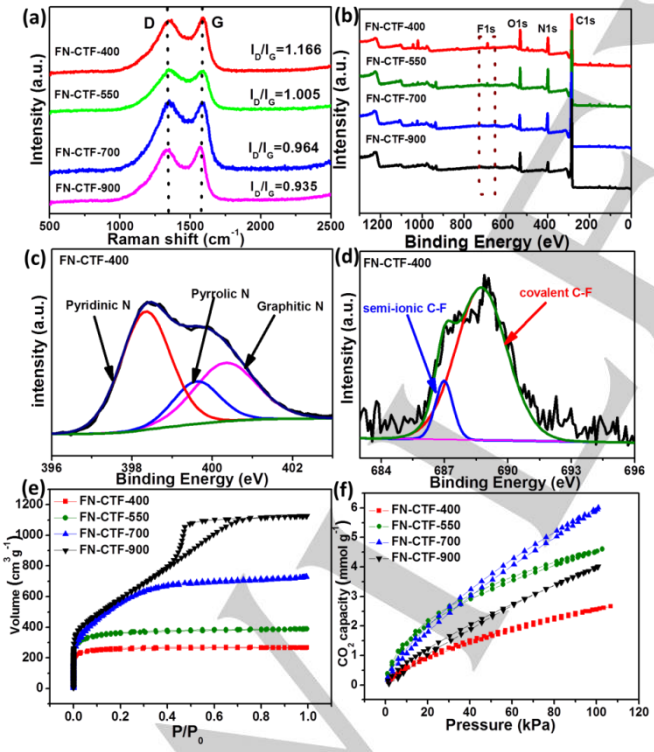

Figure 2. (a) Raman spectra and (b) XPS survey spectra of the FN-CTFs; (c) high resolution N 1s XPS spectra and (d) high resolution F 1s XPS spectra for FN-CTF-400 (e) N_2 adsorption/desorption isotherm curve and (f) CO_2 adsorption/desorption isotherm curves for FN-CTFs

The adsorption/desorption properties of gas molecules of N_2 and CO_2 are investigated by Brunauer-Emmett-Teller (BET) method. Figure 2e presents the N_2 adsorption/desorption isotherms curves for the FN-CTFs samples. The FN-CTF-900 exhibits a type-IV isothermal curve with hysteresis loop at high P/P_0 value that indicates complex micro-mesoporous structure. The other three FN-CTFs samples while feature type-I isotherm curve that imply the dominant microporous structure. The FN-CTF-400 holds a BET surface area 817 $m^2 g^{-1}$, this value is remarkably lower than those of FN-CTF-550 (1131 $m^2 g^{-1}$), FN-CTF-700 (2040 $m^2 g^{-1}$), and FN-CTF-900 (2162 $m^2 g^{-1}$), indicating more pores were produced with increasing temperature. Pore size distributions were estimated according to the adsorption branch of the nitrogen isotherms by density functional theory (DFT). The pore size distributions studies show that FN-CTF-400 and FN-CTF-550 have a major peak centered at around 0.54 nm and some other peaks below 2 nm. FN-CTF-700 has two pore size distributions at 1.2 nm and 2.8 nm, and FN-CTF-900 has a major peak centered at 0.5 nm and 4.5 nm with significantly broad distribution in the microporous and mesoporous range (Figure S6). Figure 2f presents the CO_2 adsorption/desorption isotherms curve for the set of FN-CTFs samples. All the materials have good CO_2 adsorption likely because of their surface functionalities. The sequence of the CO_2 capturing values at 1 bar for CTFs is FN-CTF-700 (6.02 mmol g^{-1}), FN-CTF-550 (4.61 mmol g^{-1}), FN-CTF-900 (4.01 mmol g^{-1}), and FN-CTF-400 (2.66 mmol g^{-1}).

The electrocatalytic properties of the CTFs samples towards CO_2 electroreduction were investigated in a closed three-electrode system with CO_2 saturated aqueous 0.1 M $KHCO_3$ solution as electrolyte. Based on cyclic voltammetry (CV) curves (Figure S7), one can observe the FN-CTF-400 shows significantly increased current density in CO_2-saturated compared with that in N_2-saturated electrolyte plus the onset potential at around -0.1 V, demonstrating the FN-CTF-400 exhibits good catalytic activity for CO_2 reduction. We further analyzed the products generated in the range of -0.4 to -1.2 V upon electrocatalysis, to this end, the gas and liquid products were monitored by gas chromatography (GC) and nuclear magnetic resonance, respectively. In this way, the catalytic selectivity of CO_2 electro-reduction can be fairly evaluated. Figures 3a-3d outline the faradaic efficiency (FE) of various CTF-based CO_2 electrocatalysts for production of CH_4, CO, and H_2, which are denoted as FE_{CH4}, FE_{CO}, and FE_{H2}, respectively. Notably, the FN-CTF-400 behaves a highly catalytic selectivity toward CO_2 electroreduction into CH_4 with a dominant competitive advantage over hydrogen evolution reaction, as evidenced by a FE_{CH4} of around 78.7% with a small FE_{H2} of below 15% in potentials between -0.4 and -0.6 V (Figure 3a). More impressively, the FE_{CH4} at FN-CTF-400 can approach up to 99.3% in the potential range of -0.7 ~ -0.9 V and gradually decrease to 65% with enhancement in FE_{H2} at potential above 1.0 V. The FN-CTF-550 exhibits a decreased selectivity for CH_4 production with a peak FE_{CH4} of ~ 62.3 % at -0.7 V and a relative high FE_{H2} of 41.6% at -0.4 V (Figure 3b). The FN-CTF-700 and the FN-CTF-900, in contrast, tend to favor catalytic conversion of H_2O and CO_2 into H_2 and CO rather than CH_4. Specifically, the FN-CTF-700 shows a peak value (58.2 %) for FE_{CO} at -0.8 V and a peak value (57.16 %) for FE_{H2} at -0.4 V (Figure 3c), and the FN-CTF-900 shows the highest value for FE_{CO} (42 %) at -0.7 V and for FE_{H2} (80 %) at -0.4 V (Figure 3d). It should be pointed

out there are no liquid hydrocarbon compound products for all FN-CTF electrocatalysts based on NMR testing reports.

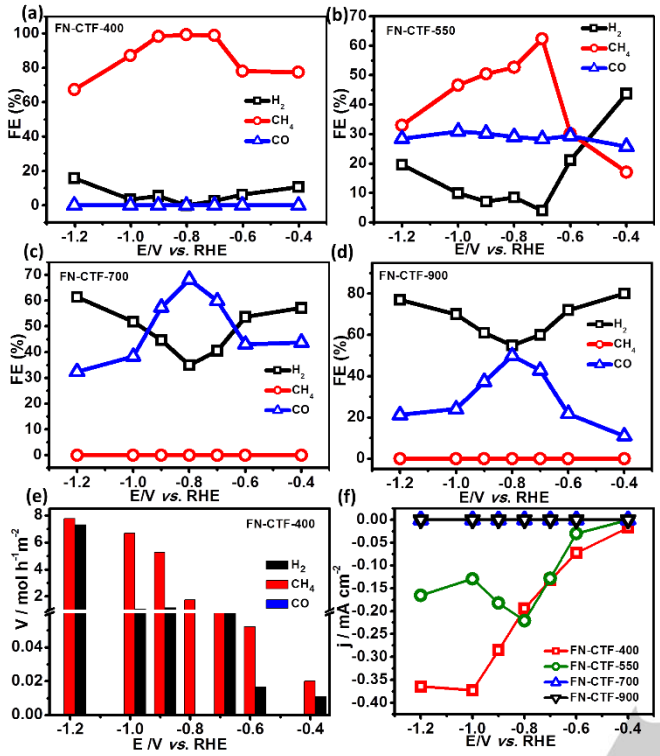

Figure 3. Faradaic efficiency for CH_4, CO and H_2 versus potential on electrodes of (a) FN-CTF-400; (b) FN-CTF-550; (c) FN-CTF-700; and (d) FN-CTF-900. (e) the production rates for H_2, CO and CH_4 at FN-CTF-400 at different applied potential; (f) current densities corresponding to CH_4 production on the set of FN-CTFs samples.

The production rates were also calculated by GC analysis of the gas production (Figure 3e and Figure S8). As expected, with increasing applied voltage, the FN-CTF-400 manifests an enhanced production rate of CH_4 from 1.05 mol h^{-1} m^{-2} at -0.7 V to 7.75 mol h^{-1} m^{-2} at -1.2 V (Figure 3e), with a much higher CH_4 production rate than that of the FN-CTFs-550 (Figure S8) and the other two FN-CTFs counterparts, which show a high production rate for either H_2 or CO (not show). Figure 3f depicts the current density regarding to CH_4 production at different potential for the set of samples. The FN-CTF-700 and the FN-CTF-900 show no CH_4 production in the potential range of -0.4 ~ -1.2 V. By contrast, the FN-CTF-400 and the FN-CTF-550 manifests a remarkable current density corresponding to CH_4 production starting at -0.4 V, and a gradual increase in current density with enhancing the applied voltage until reach a stable value at -1.2 V. Obviously, the FN-CTF-400 performs better with a much higher current density of CH_4 than the FN-CTF-550. The catalytic stability for selectively CO_2 reduction (into CH_4) was also evaluated through monitoring variation of the FE_{CH4} at intervals, the FN-CTF-400 can still maintain a FE_{CH4} of ~91.7% after 5-hours continuous running at -0.8 V (Figure S9). We conducted the electrochemical tests at FN-CTF-400 electrode in N_2 saturated electrolyte and the bare carbon paper electrode in CO_2 saturated electrolyte with monitoring the products (Figure S10), no CH_4 product is produced in both cases, verifying that the carbon in CH_4 production at FN-CTF-400 electrode in CO_2 saturated electrolyte was from CO_2 other than the catalysts or electrolyte. The electrochemical surface areas for FN-CTF-400 and the bare carbon paper were evaluated based on the double layer capacitive (C_{dl}) by cyclic voltammetry (Figure S11a and b).[9] The C_{dl} of FN-CTF-400 (965 μF cm^{-2}) is far larger than that of the bare carbon paper (3.58 μF cm^{-2}) (Figure S11c), confirming the CO_2RR activity stems from the FN-CTF-400 catalysts.

The above results evidence the FN-CTF-400 possess an impressively high catalytic selectivity toward CO_2 conversion into CH_4, it is thus desirable to study what peculiarity in FN-CTF-400 give rise to such high-selectivity catalysis. The FN-CTF-400, according to characterization and previous report,[6d,10] was likely a composite consisting of majorly polymer and small amounts of pyrolyzed carbon, because it was prepared at a relatively low temperature. The polymer in FN-CTF-400 provides desirable structureres for capturing CO_2 molecules and hydrophobic environment to suppress hydrogen evolution,[6h,11] while the F/N codped carbon offer the favorable catalytic activity sites for CH_4 production. For the other FN-CTF samples, most of the polymer structures have turned into graphite structure that tends to catalyze CO_2 reduction into CO. Besides, it is interesting to investigate the role of F-doping due to the varied F-doped level in the set of FN-CTF samples. The FN-CTF-400, which possess the highest F-doping level, indeed exhibits the highest selectivity for CO_2 electroreduction into CH_4 (*i.e.*, FE_{CH4}), followed by the FN-CTF-550 that hold the second position in F-doping level and FE_{CH4}. For both the FN-CTF-700 and the FN-CTF-900 that do not contain fluorine, they favorably catalyze reduction CO_2 into CO, rather than CH_4. It is thus rational to infer the F-doping in FN-CTF do play a key role in selectively reducing CO_2. We additionally prepare chloride containing TIF (ClN-CTF-400) with performing the associated characterization (Figure S12-14). The electrochemical measurements (Figure S15) are conducted to study its catalytic activities and selectivity, which indicates the ClN-CTF-400 also perform decently toward selectively catalyzing conversion CO_2 into CH_4 with a maximum FE_{CH4} of around 74.9 % at -0.8 V. In addition, three N-containing only CTFs (N-CTF, Figure S16-S19) were also prepared by using the same method as FN-CTF-400 with F-free materials as precursors, respectively. All the three N-CTF catalysts show a preferred CO products with a relatively low FE_{CH4} (Figure S20) and a tiny CH_4 production rate (Figure S21) over the potential range of -0.2~-1.2 V. The set of electrochemical experiments on controlled samples strongly evidence that the F-doping plays a critical role in regulating the selectivity of the product in the electrocatalysis of CO_2 reduction.

Density functional theory (DFT) calculation was performed to study why the FN-CTFs-400 electrocatalysts hold such high selectivity in conversion of CO_2 into CH_4. To this end, the computational hydrogen electrode (CHE) method proposed by Nørskov *et al* [12] was applied, in which the limiting potential (UI) was calculated to estimate the activity and selectivity (Sec 2 of supporting information). The computational models were built based on the physical characterization, where N and F -doped carbon are modeled with all the possible doping configurations in references of the former work[13] as depicted in Figure S1. The reaction pathway for CO_2 elctroreduction into CO (g) and CH_4 (g) [8] is described as RS1-RS14 (Sec. 2.2 of supporting information).

The CHO* pathway (RS4-RS8) is more likely to be the exact pathway,[7] as indicated in Figure S22. For N doping, the edge graphite N, including the single-N graphitic (gN) and pair-N graphitic (2gN), are the active sites, while for N & F co-doping, pyrrolic N site is also active for CO_2 electroreduction. Figure 4 displays the top views and the associated DFT reaction free energy diagram (FED) of the active sites for CO_2 electroreduction. Figure 4a-4b and Figure 4c-4e represent the N-CTF and NF-CTF catalysts, respectively. According to the FEDs, it is clear that, among all the active sites, only Edge-gN is more prone to produce CO, while the other four active local configurations produce CH_4: (1) Experiments illustrates the TB-CTF-400, NP-CTF-400 and NB-CTF-400 with only N-doping structures produce both CH_4 and CO (Figure S20a-S20c), based on our DFT calculations, the existence of both Edge-gN and Edge-2gN are the catalytic sites for these samples, since these two sites are responsible for the production of CO (Figure 4a) and CH_4 (Figure 4b), respectively; (2) FN-CTF-700 (Figure 3c) and FN-CTF-900 (Figure 3d) are also the N-doped structures, while the high temperature treatment impair activity of the pair-N (Edge-2gN) due to destruction, leading to that Edge-gN become the main contribution. CO accordingly becomes the main product on these two catalysts; (3) when F is covalent to the N-containing catalysts, the Edge-gN-F (Figure 4c) and Edge-2gN-F (Figure 4d) will be formed accompanying with pyrrolic N as active site upon F doping (Figure 4e). According to their FEDs (Figure 4c-4e), CH_4 will be the main products for FN-CTF-400. This matches well with the Faraday efficient diagram for FN-CTF-400, which suggests CH_4 is the main product; (4) For FN-CTF-550, some of the F would escape upon carbonization, the originally existing site Edge-gN-F in FN-CTF-400 has recovered to the F-free site Edge-gN, which is active site for the production of CO. Such correspondence to the experimental selectivity verifies the accuracy of DFT based mechanisms, revealing the key active sites and their aiming products, which could be an important guidance for strategies of synthesizing more advanced materials that possess higher selectivity and activity on CO_2RR in the future.

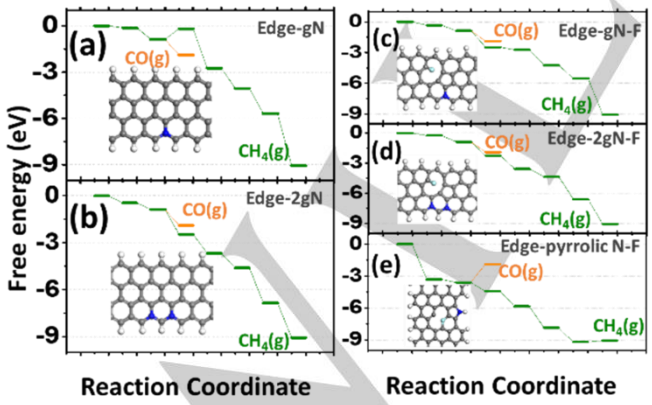

Figure 4. The reaction models for the verified active sites for N doped (a-b) and N & F co-doped (c-e) structures. The top views for the structures are shown, with C, H, N and F atoms colored by grey, white, blue and cyan. In the FEDs, the green and orange pathways indicate CO and CH_4 pathway, respectively.

In summary, we prepared a set of covalent triazine framework (CTF) catalyst with tunable the surface functionality by introducing a variety of heteroatom doping. We demonstrate the CTF with substantial F-covalent can function as a high-selectivity electrocatalyst for CO_2 electroreduction to CH_4 with a faraday efficiency of approaching 100%. The systematic electrochemical study, coupling with DFT calculation, demonstrate the ultrahigh selectivity observed for FN-CTF-400 can be attributed to the doped F which regulates the activity of N and make it more conductive to CH_4 production. This work provides an important guidance for strategies to design and synthesize advanced electrocatalysts that possess high selectivity and activity on CO_2 electroreduction.

Acknowledgements

We would like to thank 1000 Plan Professorship for Young Talents, Hundred Talents Program of FuJian Province, the Fujian Science and Technology Key Project (Item Number. 2016H0043), the National Natural Science Foundation of China (Grant No. 21703250) for financial support.

Keywords: High-selectivity electrocatalysis • CO_2 reduction• Covalent triazine framework• Catalytic sites

[1] a) M. S. Dresselhaus, Thomas, I. L. *Nature* **2001**, 414, 332-337; b) S. Chu, A. Majumdar, *Nature* **2012**, *488*, 294-303; c) J. G.Canadell, C. Le Quere, M. R. Raupach, C. B. Field, E. T. Buitenhuis, P. T. Ciais, J. Conway, N. P. Gillett, R. A. Houghton, G. Marland , *Proc. Natl. Acad. Sci. USA.* **2007**, 104, 18866-18870; d) D. D. Zhu, J. L. Liu, S. Z. Qiao, *Adv. Mater.* **2016**, *28*, 3423-3452.

[2] a) R. F.Service, *Science* **2010**, 327, 257-257; b) N. Kornienko, Y. Zhao, C. S. Kiley, C. Zhu, D. Kim, S. Lin, C. J. Chang, O. M. Yaghi, P. Yang, *J. Am. Chem. Soc.* **2015**, *137*, 14129-14135; c) F. Li, M. Xue, J. Li, X. Ma, L. Chen, X. Zhang, D. R. MacFarlane, J. Zhang, *Angew. Chem.Int. Ed.* **2017**, *56*, 14718-14722; d) M. Asadi, K. Kim, C. Liu, A. V.Addepalli, P. Abbasi, P. Yasaei, P. Phillips, A. Behranginia, J. M. Cerrato, R. Haasch, P. Zapol, B. Kumar, R. F. Klie, J. Abiade, L. A. Curtiss, A. Salehi-Khojin, *Science* **2016**, 353, 467-470..

[3] a) S. Lin, C. S. Diercks, Y.-B. Zhang, N. Kornienko, E. M. Nichols, Y. Zhao, A. R. Paris, D. Kim, P. Yang, O. M. Yaghi, C. J. Chang, *Science* **2015**, *349*, 1208-1213; b) F. Li, L. Chen, G. P. Knowles, D. R. MacFarlane, J. Zhang, *Angew.Chem.Int. Ed.* **2017**, *56*, 505-509; c) C. S. Diercks, Y. Liu, K. E. Cordova, O. M. Yaghi, *Nat. Mater.* **2018**, *17*, 301-307.

[4] a) Y. Zhang, L. Chen, F. Li, C. D. Easton, J. Li, A. M. Bond, J. Zhang, *ACS Catal.* **2017**, *7*, 4846-4853; b) H. Mistry, R. Reske, Z. Zeng, Z. J. Zhao, J. Greeley, P. Strasser, B. R. Cuenya, *J. Am. Chem. Soc.* **2014**, *136*, 16473-16476; c) R. Reske, H. Mistry, F. Behafarid, B. Roldan Cuenya, P. Strasser, *J. Am. Chem. Soc.* **2014**, *136*, 6978-6986; d) W. Zhu, R. Michalsky, O. Metin, H. Lv, S. Guo, C. Wright, X. Sun, A. A. Peterson, S. Sun, *J. Am. Chem. Soc.* **2017**, *139*, 9408-9408; e) M. Liu, Y. Pang, B. Zhang, P. De Luna, O. Voznyy, J. Xu, X. Zheng, C. T. Dinh, F. Fan, C. Cao, F. P. de Arquer, T. S. Safaei, A. Mepham, A. Klinkova, E. Kumacheva, T. Filleter, D. Sinton, S. O. Kelley, E. H. Sargent, *Nature* **2016**, *537*, 382-386.

[5] a) P. Kuhn, A. Forget, D. Su, A. Thomas, M. Antonietti, *J. Am. Chem. Soc.* **2008**, 130, 13333-13337; b) R. Dawson, A. I. Cooper, D. J. Adams, *Prog. Polym. Sci.* **2012**, *37*, 530-563; c) A. Thomas, *Angew. Chem. Int. Ed.* **2010**, *49*, 8328-8344; d) Y. Xu, S. Jin, H. Xu, A. Nagai, D. Jiang, *Chem. Soc. Rev.* **2013**, *42*, 8012-8031.

[6] a) J. Schmidt, J. Weber, J. D. Epping, M. Antonietti, A. Thomas, *Adv. Mater.* **2009**, *21*, 702-705; b) S. Yang, Y. Gong, J. Zhang, L. Zhan, L. Ma, Z. Fang, R. Vajtai, X. Wang, P. M. Ajayan, *Adv. Mater.* **2013**, *25*, 2452-2456; c) A. P. Cote, A. I. Benin, N. W. Ockwig, M. O'Keeffe, A. J. Matzger, O. M. Yaghi, *Science* **2005**, *310*, 1166-1170; d) L. Hao, X. Li, L. Zhi, *Adv. Mater.* **2013**, *25*, 3899-3904; e) Y. Kou, Y. Xu, Z. Guo, D. Jiang, *Angew. Chem. Int. Ed.* **2011**, *123*, 8912-8916; f) L. Hao, S. Zhang, R. Liu, J. Ning, G. Zhang, L. Zhi, *Adv. Mater.* **2015**, *27*, 3190-3195; g) P. Kuhn, M. Antonietti, A. Thomas, *Angew. Chem. Int. Ed.* **2008**, *47*, 3450-3453; h) Y. Zhao, K. X. Yao, B. Teng, T. Zhang, Y. Han, *Energy Environ. Sci.* **2013**, *6*, 3684-3692.

[7] J. Yang, X. Zhou, D. Wu, X. Zhao, Z. Zhou, *Adv. Mater.* **2017**, *29*.

[8] S. Fu, C. Zhu, J. Song, M. Engelhard, B. Xiao, D. Du, Y. Lin, *Chem. Eur. J.* **2017**, 23,10460-10464.

[9] C. Tang, R. Zhang, W. B. Lu, Z. Wang, D. N.Liu, S. Hao, G. Du, A. M. Asiri, X. P. Sun, *Angew. Chem. Int. Ed.* **2017**, *129*, 860-864.

[10] P. Kuhn, A. Thomas, M. Antonietti, *Macromolecules*, **2009**, 42, 319-326

[11] X. Zhu, C. C. Tian, G. M. Veith, C. W. Abney, J. Dehaudt, S. Dai, *J. Am. Chem. Soc*., **2016**, 138, 11497-11500.

[10] a) J. K. Norskov, J. Rossmeisl, A. Logadottir, L. Lindqvist, J. R. Kitchin, T. Bligaard, H. Jonsson, *J. Phys.Chem. B* **2004**, *108*, 17886-17892; b) A. A. Peterson, F. Abild-Pedersen, F. Studt, J. Rossmeisl, J. K. Norskov, *Energy Environ. Sci.* **2010**, *3*, 1311-1315; c) A. A. Peterson, J. K. Norskov, *J. Phys. Chem. Lett.* **2012**, *3*, 251-258.

[11] a) G.-L. Chai, Z.-X. Guo, *Chem. Sci.* **2016**, *7*, 1268-1275; b) M. Wu, C. Cao, J. Z. Jiang, *Nanotechnology* **2010**, *21*.

10.1002/anie.201807173

WILEY-VCH

Entry for the Table of Contents (Please choose one layout)

Layout 1:

COMMUNICATION

Text for Table of Contents

The F-containing COF materials shows an unprecedented high selectivity with faradaic efficiency of 99.3% toward electrochemical conversion of carbon dioxide into CH_4. DFT calculation demonstrates that co-covalent of nitrogen and fluorine contributes the catalytic sites for CH_4 production.

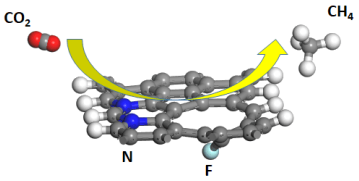

Yuanshuang Wang [a] +, Junxiang Chen [a] +Genxiang Wang[a] +, Yan Li[a] and Zhenhai Wen[a]*

Page No. – Page No.

Perfluorinated Covalent Triazine-based Framework as High-selectivity Electrocatalysts for Conversion CO_2 into CH_4